

Mobile and Immobile Obstacles in Supported Lipid Bilayer Systems and Their Effect on Lipid Mobility

Luisa Coen, Daniel Alexander Kuckla, Andreas Neusch and Cornelia Monzel *

Experimental Medical Physics, Heinrich-Heine University, 40225 Düsseldorf, Germany

* Correspondence: cornelia.monzel@hhu.de; Tel.: +49-(0)21181 - 12893

SUPPORTING INFORMATION

1. Theory

1.1 Diffusion in Biological Membranes

The first theoretical model to calculate the diffusion constant of proteins in lipid membranes, proposed by Saffman and Delbrück, models the lipid membrane as an infinitely flat sheet of a homogeneous, viscous fluid. The model ignores the complex nature of the bilayer, which is naturally composed of various phospholipids, glycolipids, cholesterol, and proteins. Membrane proteins are represented as cylinders embedded in this viscous fluid with the symmetry axes pointing perpendicular to the membrane surface and without any molecular parts extending above or below the membrane. The diffusion constant of the membrane fluid is, in this case, logarithmically dependent on the size of the membrane embedded moiety [54]:

$$D = \frac{\overline{r^2}}{4t} = \frac{k_B T}{4\pi\eta h} \cdot \left(\log\left(\frac{\eta h}{\eta' a}\right) - \gamma \right), \quad (\text{Eq. S1})$$

where $\overline{r^2}$ is the mean square displacement, t the time, k_B the Boltzmann constant, T the temperature, η the viscosity of the fluid representing the membrane, η' the viscosity of the surrounding fluid, h the height of the lipid membrane, a the radius of the diffusing particle, and γ the Euler constant. As a first approximation, **Eq. S1** can also be used to calculate the diffusion constant of lipids. One extension of this theory is given by Petrov and Schwille. They expanded the Saffman and Delbrück model to consider larger membrane inclusions as obstacles [56].

1.2 Friction Between SLB and Substrate

In the case of SLBs, the interaction between the solid and the membrane results in an additional source of friction, which reduces the mobility within the membrane. Here, the theory of Evans and Sackmann introduces inertia-lacking equations of motion for objects in a fluid SLB and assumes proportionality between interfacial shear stress and membrane velocity. In this model, the friction coefficient of the moving object, b , is the key parameter to calculate the diffusion constant [57]:

$$D = \frac{k_B T}{4\pi\eta_m} \left(\frac{1}{4} \varepsilon^2 + \frac{\varepsilon K_1(\varepsilon)}{K_0(\varepsilon)} \right)^{-1}. \quad (\text{Eq. S2})$$

Here, η_m is the membrane surface viscosity, and K_1 and K_0 are the modified Bessel functions of second kind and first or zeroth order. ε is the dimensionless particle radius given by [57]:

$$\varepsilon = a \cdot \sqrt{\frac{b}{\eta_m}}, \quad (\text{Eq. S3})$$

with a as the real particle radius, and b as the friction parameter.

For low friction, the Saffman/Delbrück result is recovered, whereas for high friction, the diffusion coefficient depends strongly on the size of the diffusing particle. In our study, both the tracers and the proteins can be interpreted as diffusing particles, which is considered a disc-like particle, without further assumption. For this reason, the Evans/Sackmann model is well-suited to compare friction parameters between the different model systems. Like Saffman/Delbrück, the Evans/Sackmann description ignores the discrete nature of the bilayer.

It should be noted that the Saffman/Delbrück and Evans/Sackmann models consider membrane-spanning probes, which were not present in our sample. Instead, lipids or lipids with proteins coupled to the membrane were present in the upper membrane leaflet. This setup was chosen on purpose to allow for an accurate estimate of obstacle concentrations. Moreover, membrane-spanning probes were shown to contribute additional friction due to interactions with the substrate [86,87] and would require the use of a polymer cushion beneath the SLB. Since a polymer cushion would increase the system complexity and, since for polymer cushions, the tethering was reported to yield an immobile fraction [45], this approach was not considered in this work. Nonetheless, a previous study points to an epitactic coupling between the lipids in both membrane layers [58]; therefore, some membrane-spanning effects may also arise in our case.

1.3 Friction Due to Mobile Obstacles

To deal with the variable nature of the membrane components, theories accounting for friction effects arising from mobile obstacles within the membrane have been developed [60,61]. The obstacles can be individual proteins or protein clusters on the membrane surface that diffuse more slowly with increasing size, thereby influencing the diffusion of the lipids in the membrane. In Saxton's theory, diffusion is considered as a random motion on a two-dimensional grid. Obstacles and particular lipids in the membrane, so-called tracers, are randomly distributed on the grid and can jump to adjacent free places. The relative jump rate γ is defined as the ratio of the jump rate of the tracers T to the jump rate of the obstacles H: $\gamma = \gamma_T/\gamma_H$. In addition, the diffusion constant of the lipids depends on the concentration of the obstacles c , which is given as an area fraction defined by: $\left(1 + \frac{a_l n_l}{a_o n_o}\right)^{-1}$, with a_l as the area of the lipid, a_o the effective area of the obstacle, and n_l/n_o , the molar ratio of lipid to obstacle. The relative diffusion constant $D^*(c) = D(c)/D(0)$ is defined with $D(c)$ and $D(0)$ as the diffusion constants of the tracer lipid in the presence and absence of obstacles, respectively. Next to its dependence on obstacle concentration, the relative diffusion constant is also a function of the relative jump rate [60]:

$$D^*(c, \gamma) = (1 - c) \cdot \frac{\{[(1-\gamma)(1-c)f_0 + c]^2 + 4\gamma(1-c)f_0^2\}^{1/2} - [(1-\gamma)(1-c)f_0 + c]}{2\gamma(1-c)f_0}. \quad (\text{Eq. S4})$$

and

$$f_0 = \frac{1-\alpha}{1+(2\gamma-1)\cdot\alpha}. \quad (\text{Eq. S5})$$

Here, α is a lattice-dependent constant. For a square lattice $\alpha = 1 - \frac{2}{\pi}$, for a triangular lattice $\alpha = 0.282$, and $\alpha = 0.500$ for a honeycomb lattice. Using Monte Carlo simulations, Saxton was able to show that the relative diffusion constant is independent of the choice of the lattice; therefore, a triangular lattice was used in this study [60].

2. Supplementary Figures

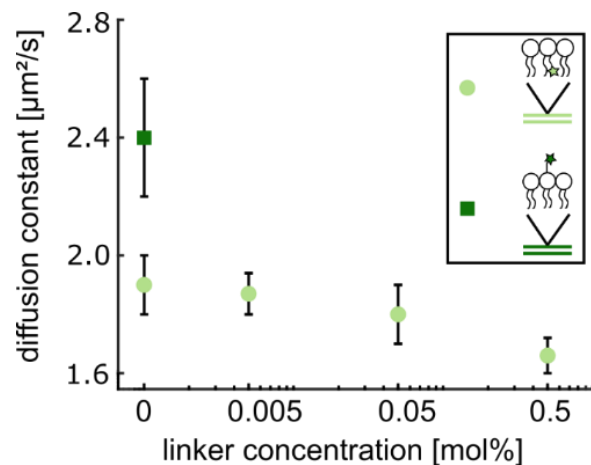


Figure S1. Fatty acid-labeled tracer. Diffusion constants for the NTA-GFP system. DOGS-NTA concentrations of 0 mol%, 0.005 mol%, 0.05 mol%, and 0.5 mol% were used. SLB with fatty acid-labeled tracer (circle), SLB with headgroup-labeled tracer (box). Data points are median \pm MAD.

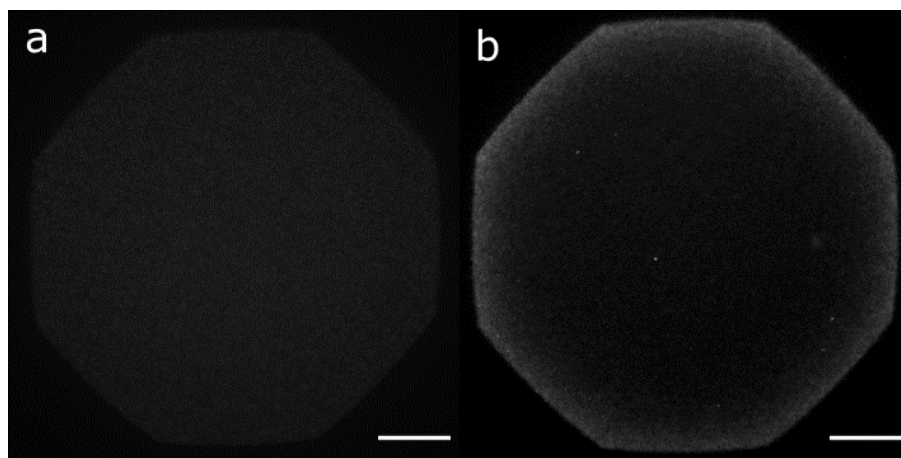


Figure S2. SLB with bound protein after bleaching. (a) NTA-GFP system. The missing bright ring at the aperture edge after bleaching indicates the immobilization of GFP. (b) Biotin-NAVOG system. The bright ring at the aperture edge after bleaching indicates the mobility of NAVOG. Scale bar in (a) and (b): 25 μ m.

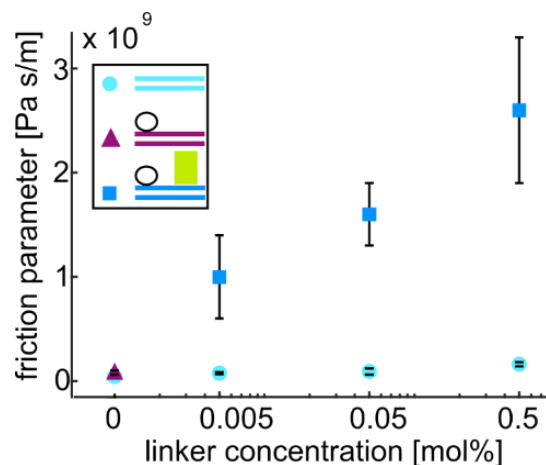


Figure S3. Calculated friction parameter for the NTA–GFP system. DOGS-NTA concentrations of 0 mol%, 0.005 mol%, 0.05 mol%, and 0.5 mol% were used. SLB alone (circle), SLB after BSA incubation (triangle), SLB after BSA passivation and GFP coupling (box). Data points are median \pm MAD.

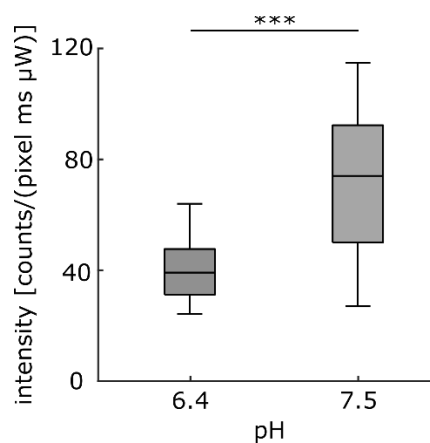


Figure S4. GFP intensity changes after incubation on the SLB at 0 mol% linker concentration as a function of pH. The intensity increase from pH 6.4 to pH 7.5 is an indicator of the charge-dependent interaction between GFP and SLB. Significance was tested via Wilcoxon rank-sum test with n.s.: $p > 0.05$, *: $p \leq 0.05$, **: $p \leq 0.01$, ***: $p \leq 0.001$. Confocal images of the SLB were taken with an Abberior Confocal Microscope (Abberior Instruments GmbH, Göttingen, Germany) equipped with a 100x objective with NA 1.4 from Olympus. The system has previously been described in detail [88].

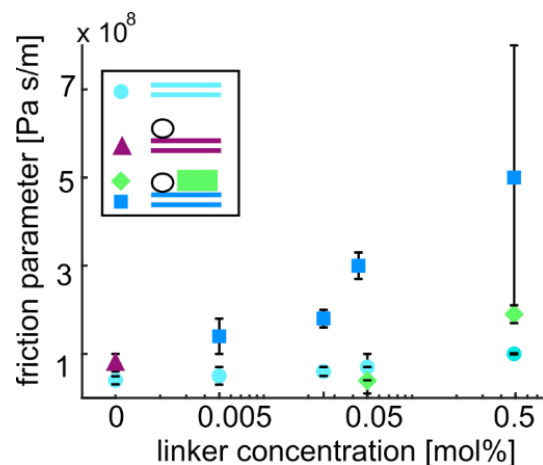


Figure S5. Calculated friction parameter for the Biotin–Neutravidin system. DOPE-Cap-Biotin concentrations of 0 mol%, 0.005 mol%, 0.05 mol%, and 0.5 mol% were used. SLB alone (circle), SLB after BSA incubation (triangle), SLB after BSA passivation and NAVOG coupling (box), NAVOG (diamond). Data points are median \pm MAD.

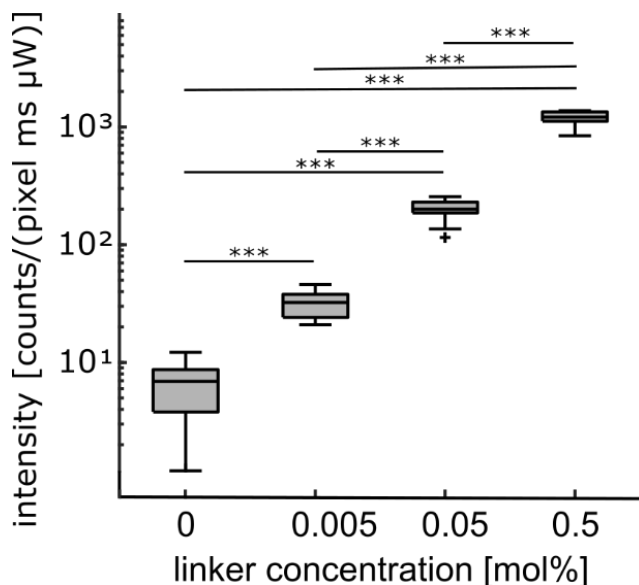


Figure S6. NAVOG intensity changes as a function of the linker concentration of the Biotin–Neutravidin system. DOPE-Cap-Biotin concentrations of 0 mol%, 0.005 mol%, 0.05 mol%, and 0.5 mol% were used. Significance was tested via Wilcoxon rank-sum test with n.s.: $p > 0.05$, *: $p \leq 0.05$, **: $p \leq 0.01$, ***: $p \leq 0.001$. The linear intensity detection with increasing fluorophore concentration was checked. Confocal images of the SLB were taken with an Abberior Confocal Microscope (Abberior Instruments GmbH, Göttingen, Germany) equipped with a 100x objective with NA 1.4 from Olympus. The system has previously been described in detail [88]. Here, a near linear increase was found with a tenfold linker concentration increase and a corresponding sixfold NAVOG intensity increase.

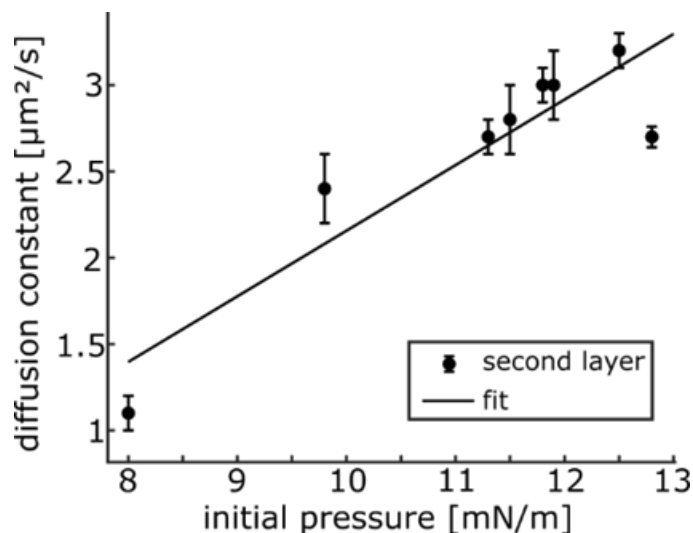


Figure S7. Calibration data for the initial pressure correction for the Biotin–Neutravidin–Actin system. Data in the graph were acquired from a linker-free SLB with 2 mg/ml SOPC + 2.5 mol% Cy5. Linear fit with y-intercept = -1.6 and slope = 0.4. The diffusion constant exhibited a dependency on the initial pressure of the second layer of the SLB. The first layer did not exhibit any pressure dependency. For this reason, diffusion constants were corrected to an initial lateral pressure value of 8 mN/m, which was the SLB fabrication pressure of the second layer in the Biotin–Neutravidin system. Data points are median \pm MAD.

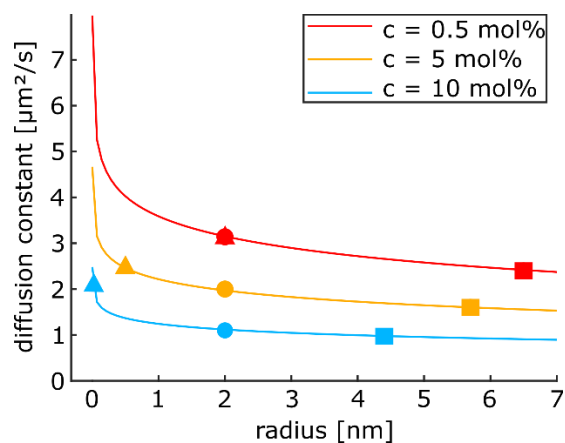


Figure S8. Diffusion constant as a function of obstacle radius for linker concentrations of 0.5 mol% (red), 5 mol% (yellow), and 10 mol% (blue). Lines represent the theory of Petrov and Schwill [56]. The theory depends on the membrane viscosity and the particle radius as parameters. To fix the membrane viscosity, the obstacle size derived from Saxton's theory ($a_0 = 12 \text{ nm}^2$, i.e. radius = 1.95 nm) for the SOPC + NAVTMR model system and all concentrations is used. The diffusion constants of the matrix lipid for pure SOPC (triangle), SOPC + NAVTMR (circle), and SOPC + NAVTMR + actin (square) are inserted into the graph to yield the obstacle radii. The theory gives reasonable obstacle radii for actin-coupled obstacles of 4.4 nm to 6.5 nm size. However, it should be noted that these values are a rough estimate based on the result of Saxton's theoretical approach.

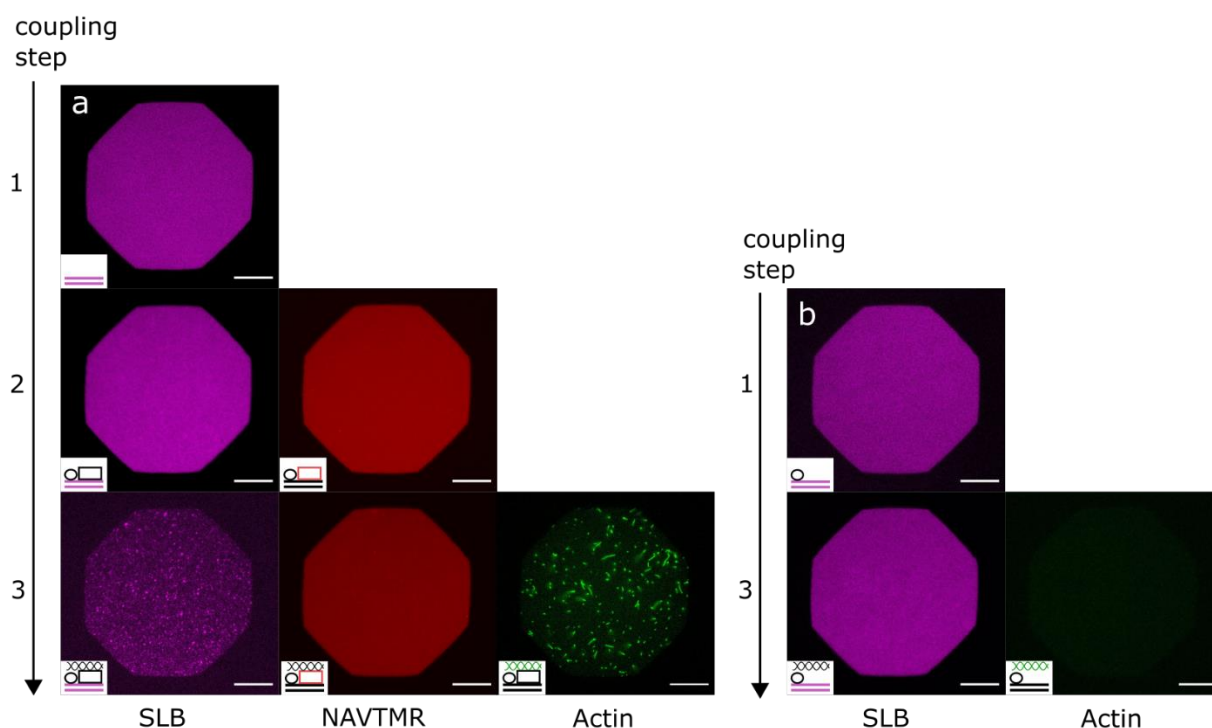


Figure S9. Representative images of the SLB before and after coupling of proteins. Different coupling steps: (1) before coupling, (2) after coupling of NAVTMR, and (3) after coupling of actin. (a) Experiment with all incubation steps; (b) control measurement without NAVTMR but with actin incubated. Linker concentration in (a) and (b): 5 mol%. Scale bars: 25 μm .

SUPPLEMENTARY REFERENCES

45. Deverall, M.A.; Gindl, E.; Sinner, E.K.; Besir, H.; Ruehe, J.; Saxton, M.J.; Naumann, C.A. Membrane Lateral Mobility Obstructed by Polymer-Tethered Lipids Studied at the Single Molecule Level. *Biophys J* **2005**, *88*, 1875–1886, doi:10.1529/biophysj.104.050559.
54. Saffman, P.G.; Delbrueck, M. Brownian Motion in Biological Membranes. *Proc Natl Acad Sci U S A* **1975**, *72*, 3111–3113, doi:10.1073/PNAS.72.8.3111.
56. Petrov, E.P.; Schwille, P. Translational Diffusion in Lipid Membranes beyond the Saffman-Delbrück Approximation. *Biophys J* **2008**, *94*, L41, doi:10.1529/BIOPHYSJ.107.126565.
57. Evans, E.; Sackmann, E. Translational and Rotational Drag Coefficients for a Disk Moving in a Liquid Membrane Associated with a Rigid Substrate. *J Fluid Mech* **1988**, *194*, 553–561, doi:10.1017/S0022112088003106.
58. Merkel, R.; Sackmann, E.; Evans, E. Molecular Friction and Epitactic Coupling between Monolayers in Supported Bilayers. *Journal de Physique* **1989**, *50*, 1535–1555, doi:10.1051/JPHYS:0198900500120153500.

60. Saxton, M.J. Lateral Diffusion in an Archipelago. The Effect of Mobile Obstacles. *Biophys J* **1987**, *52*, 989–997, doi:10.1016/S0006-3495(87)83291-5.
61. Saxton, M.J. Anomalous Diffusion Due to Obstacles: A Monte Carlo Study. *Biophys J* **1994**, *66*, 394–401.
86. Sackmann, E.; Tanaka, M. Supported Membranes on Soft Polymer Cushions: Fabrication, Characterization and Applications. *Trends Biotechnol* **2000**, *18*, 58–64, doi:10.1016/S0167-7799(99)01412-2.
87. Pace, H.; Simonsson Nyström, L.; Gunnarsson, A.; Eck, E.; Monson, C.; Geschwindner, S.; Snijder, A.; Höök, F. Preserved Transmembrane Protein Mobility in Polymer-Supported Lipid Bilayers Derived from Cell Membranes. *Anal Chem* **2015**, *87*, 9194–9203, doi:10.1021/ACS.ANALCHEM.5B01449.
88. Bartels, N.; van der Voort, N.T.M.; Opanasyuk, O.; Felekyan, S.; Greife, A.; Shang, X.; Bister, A.; Wiek, C.; Seidel, C.A.M.; Monzel, C. Advanced Multiparametric Image Spectroscopy and Super-Resolution Microscopy Reveal a Minimal Model of CD95 Signal Initiation. *Sci Adv* **2024**, *10*, 3238, doi:10.1126/sciadv.adn3238.